UNIVERSITY of
BRADFORD

Library

The University of Bradford Institutional Repository

http://bradscholars.brad.ac.uk

This work is made available online in accordance with publisher policies. Please refer to the repository record for this item and our Policy Document available from the repository home page for further information.

To see the final version of this work please visit the publisher's website. Access to the published online version may require a subscription.

Flexural behaviour of asymmetric composite beam with low degree of shear connection

Therese Sheehan*, Xianghe Dai and Dennis Lam

School of Engineering, University of Bradford, Richmond Road, Bradford BD7 1DP, United Kingdom

Abstract

This paper outlines an experiment on a 12 m long composite beam subjected to uniformly distributed loading. Although composite beams are widely used, current Eurocode design guidelines for these types of members can be over-conservative, particularly in relation to the required degree of shear connection. The tested beam comprised a concrete slab supported by profiled metal decking, connected to an asymmetric fabricated steel I-beam using welded shear studs. The specimen was assembled using unpropped construction methods and had a degree of shear connection equal to 33%, significantly lower than the minimum required amount specified in Eurocode 4. A uniformly distributed load was applied to the specimen, which was increased until the failure occurred characterized by yielding of the steel beam. The maximum bending moment of the composite beam obtained from the test was close to the plastic bending resistance according to the Eurocode 4. No concrete crushing or shear stud failure was observed and the end slips exceeded 6 mm, the limit for ductile behaviour in Eurocode 4. The test demonstrated the merits of unpropped construction, which are currently not fully exploited in Eurocode 4. The comparison and analysis suggest that the design limits governing the minimum degree of shear connection might be revised.

Keywords: composite beams; shear connection; unpropped construction; Eurocode 4

1 Introduction

Steel-concrete composite beams are widely used in construction, since they can span large distances without intermediary supports and have a considerable load-carrying capacity. The beam, which typically consists of a concrete slab on top of a steel I-section, achieves composite action through the use of shear connectors, which are welded onto the steel and embedded in the concrete. When the composite beam is subjected to bending, the concrete slab contributes to resisting the compressive stresses in the upper portion of the cross-

section, and thus asymmetric steel beams are sometimes used, in which the top flange has a smaller cross-sectional area than the bottom flange. The ratio of the bottom to top flange areas is usually in the range of 1.5 to 2.5 in construction practice. A higher degree of shear connection is required for asymmetric beams than for symmetric beams in Eurocode 4 (2004) (nearly 100%) and this is very difficult to achieve, since the number of shear connectors is limited by the spacing of the deck ribs (usually 300 mm for trapezoidal decking). Therefore design is often governed by achieving the minimum degree of shear connection.

The response of composite beams is influenced by the construction methods. Temporary props can be employed during construction to support the weight of the steel beam and the wet concrete slab. These props are removed once the concrete has hardened and gained sufficient strength, at which stage the composite section supports its self-weight. If props aren't used during the concrete casting, this weight is supported by the steel beam alone. Unpropped construction can reduce the construction time and can be beneficial to the performance of the shear studs: under the weight of the wet concrete, the steel beam bends and the shear studs are free to move within the wet concrete as the beam rotates. On the other hand, in the case of propped construction, the concrete has hardened before the beam has to support its own weight, and hence the studs are subjected to stresses when they follow the beam rotation. According to Lawson and Saverirajan (2011) and Banfi (2005), unpropped beams experience a lower degree of end-slip and require a lower degree of shear connection. The advantages associated with using unpropped construction method are not currently exploited in Eurocode 4 (2004).

Extensive research has been conducted to date on composite beams. Ranzi et al. (2009) carried out full scale tests on composite beams with deep trapezoidal decking. Lam (2007) examined the resistance of headed shear studs when used in composite beams in conjunction with precast hollow core slabs. Qureshi et al. (2011) considered the effect of shear connector spacing and configuration on their capacity. Zona and Ranzi (2014) examined the slip demand on shear connectors using a numerical model. Seracino et al. (2001) developed a method to predict the flexural stresses and strain distribution for composite beams with partial shear connection. Some researchers, such as Papastergiou and Lebet (2014) and Luo et al (2012) have explored the bond between steel and concrete using alternative methods to shear studs, e.g. adhesives. In recent years, the focus has shifted to a new type of composite beam: the composite cellular beam.

Cellular beams offer a reduction in self-weight and increase in section depth in comparison with solid-web beams. Some experiments have been carried out to date on non-composite, steel cellular beams, such as that by Erdal and Saka (2013) and Durif et al. (2013) but few studies exist to date that consider composite cellular beams. Lawson et al. (2006) considered the design rules for composite asymmetric cellular beams and verified these rules using finite element analysis. Sheehan et al. (2016) conducted a test on a 15.3 m long composite cellular beam using unpropped construction and a low degree of shear connection. The beam resisted over 3 times the design working load and exhibited sufficient ductile shear connector behaviour.

In order to address some of these issues, two composite beams were tested in the University of Bradford, UK as part of the European research project "Development of Improved Rules for Shear Connection in Composite Beams (DISCCO)". The main purpose of these tests were to investigate:

• The ability of the concrete steel composite beam to develop its plastic bending resistance with low degrees of shear connection (less than the required limit given in the Eurocode 4, 2004);

• The effect of un-propped construction on the longitudinal shear connector forces;

• The difference in response between the solid-web and cellular beams

The first beam tested was a 15.3 m long composite asymmetric cellular beam which has been reported by Sheehan et al. (2016). This paper will report the second beam test, an 11.2 m long solid web composite beam.

2   Beam details

2.1   Geometry

The beam consisted of a fabricated 450 mm deep I-section, with top flange dimensions of 180 × 10 mm, bottom flange dimensions of 180 × 15 mm and web dimensions of 425 × 10 mm, as shown in Figure 1. The beam was 12 m long with a span of 11.2 m between the supports. The ratio of the top flange area to the bottom flange area was 1:1.5. A trapezoidal deck profile was used to support the concrete slab, which was 80 mm deep and 0.9 mm thick with a 15 mm re-entrant stiffener on the top. The deck ribs ran in the

transverse direction to the beam length and had a spacing of 300 mm. A single 19 mm diameter shear stud was welded to the top flange of the beam through each rib to transfer the shear forces between the concrete slab and steel beam. The concrete slab was 2800 mm wide and 150 mm deep.
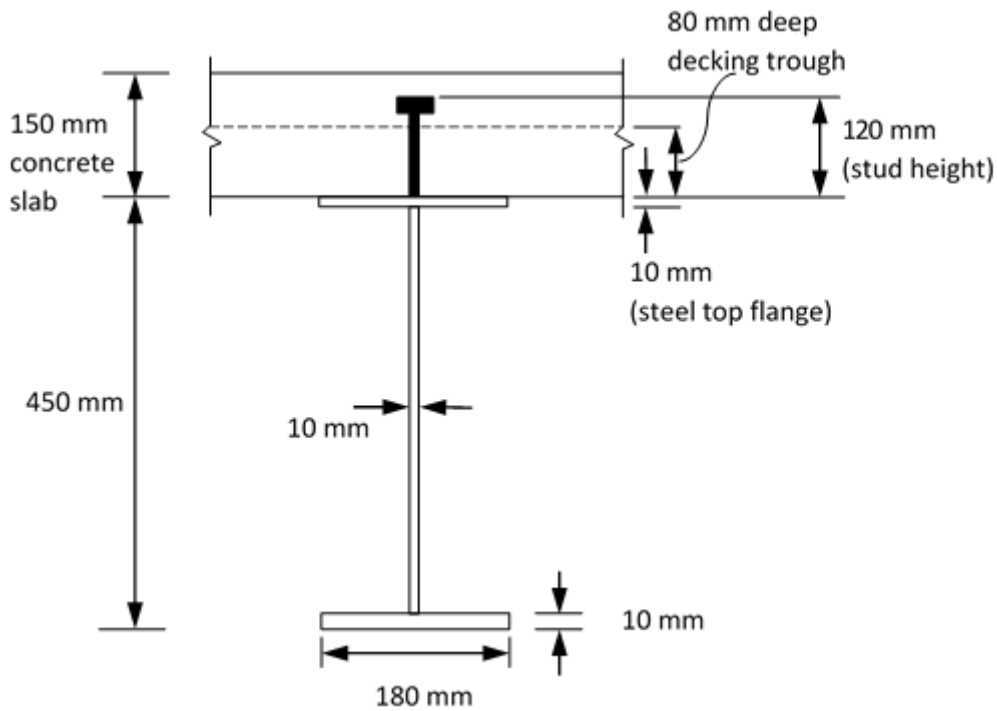

Fig. 1 Fabricated beam cross-sectional dimensions

2.2   Material properties

Grade S355 steel was used for the steel beam. The 10 mm thick plate used for the top flange and web had a measured yield stress of 440 N/mm^2 and the 15 mm thick plate for the bottom flange has a measured yield stress of 400 N/mm^2. The concrete design strength was 30 N/mm^2 but as the tests were to be carried out within 28 days of the casting (26 days), it was anticipated that the concrete would not have reached its full strength by the test date. The compressive strength of the concrete was found to be 25 MPa. This was the average result from tests carried out on three cube samples. Based on previous tests, the capacity of the shear studs was assumed to be 70 kN.

2.3   Specimen preparation

Figure 2 shows the steel beam resting on simple supports at the beginning of the specimen preparation. In order to achieve the unpropped construction conditions, similar to those commonly encountered on site, a system of wing beams was used to support the decking during casting. This system had previously been employed for the composite cellular beam test described by Sheehan et al. (2016). IPE 200 sections were bolted onto the web of the beam at 6 locations along the length. Attached to the other end of these sections were channel sections running in the longitudinal direction, which supported the weight of the concrete and steel decking. The longitudinal and 'wing' beam system transferred the weight of the decking system back to the beam, and was removed after the concrete had gained its design strength.

Once the wing beams were in place, the decking was installed as shown in Figure 3 and a single row of shear studs was welded at 300 mm spacings at the deck along the beam length. Following this, a layer of A193 mesh reinforcement (comprising a 200 mm × 200 mm grid of 7 mm diameter wire) was placed upon the deck before the concrete was poured. After 14 days, once the concrete had sufficient strength, the wing beam system was removed.

During the casting of the concrete, the deflection of the beam under the weight of the concrete was measured in two stages: the first stage was during the pouring of the concrete, while the decking and 'wing' system were supported by props. Very small deflections were observed at this stage. After the casting, the props were removed and the beam underwent larger deflections under the weight of the concrete. The total beam deflection under the weight of the concrete was obtained by adding the deflections measured from these two stages. Figure 4 shows the deflections at each stage and the total deflection along the beam length. The maximum deflection at the mid-span was 23 mm, which was slightly lower than the theoretical prediction of 26 mm. One possible explanation for this difference is that the wing beams contributed to the bending resistance of the section.

The maximum strains measured in the top and bottom flanges of the steel beam during concrete pouring were -401 and 365 $\mu\varepsilon$ respectively, both of which are significantly lower than the yield strain of the steel.

Fig. 2 Fabricated beam with 'wing' beam system

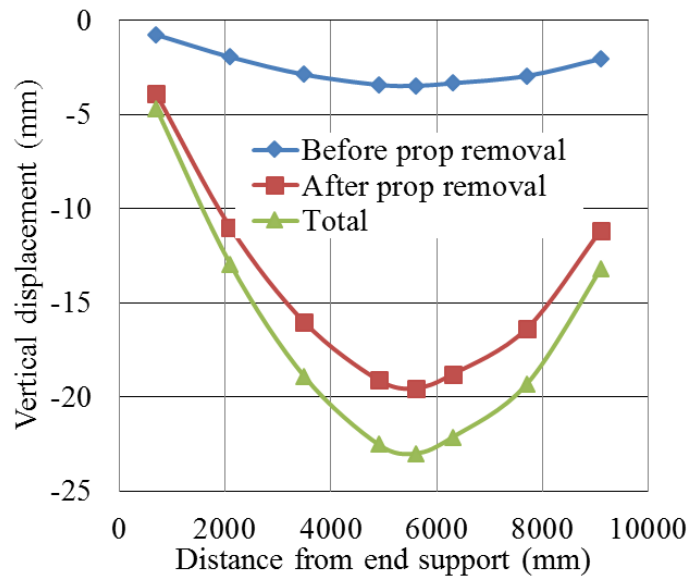Fig. 3 Welding of shear studs to the steel beam flange through the decking

Fig. 4 Vertical deflection of beam during concrete casting

2.4 Testing

2.4.1 Test set-up

The load was applied at eight evenly spaced points along the beam to mimic uniform loading, in the same manner as for the cellular beam test conducted by Sheehan et al. (2016). The loading arrangement, using one 250-tonne and two 100-tonne hydraulic actuators, is shown in Figure 5. The specimen was to be subjected the following sequence of cycles:

- Applied load up to 3 kN/m^2 (excluding self-weight of specimen and spreader beams)

- Applied load up to 5 kN/m^2 (the design working load)

- Applied load up to 7.5 kN/m^2

- Applied load up to 10 kN/m^2

- Applied load up to 12 kN/m^2

- Applied load up to 15 kN/m^2

- Applied load up to failure

2.4.2 Instrumentation

15 LVDTs were used to monitor displacements of the beam. Nine of these (LVDTs 1 – 9) were placed underneath to measure the vertical deflections. One LVDT was placed at each end (LVDTs 10 and 11) to measure longitudinal slip between the concrete slab and the steel beam. The remaining 4 (LVDTs 12 – 15)

recorded the relative slip between the steel decking and steel beam, and were located close to the 2nd and 5th shear studs from each end. The arrangement and numbering of LVDTs is presented in Figure 6.

20 strain gauges were used to monitor strains on the steel beam. Cross-sections at 6 locations along the beam length were selected for strain monitoring, as shown in Figure 6. The positions of strain gauges on the cross –section and numberings of these are illustrated in this figure. Most of the strain gauges were located within 700 mm of the midspan, measuring strains on the top flange, bottom flange and web. Strains in the top flange were also measured at 2100 mm and 3500 mm from the midspan and in the bottom flange at 2100 mm, 3500 mm and 4900 mm from the mid-span. 4 strain gauges were used to measure the longitudinal strain on the top face of the concrete at the mid-span.

3 Experimental results

3.1 Vertical deflection at the mid-span

The mid-span vertical deflection, measured by LVDT-5, is presented for each cycle of the test in Table 1. A residual deflection was observed at the end of each loading cycle, which increased with progressive cycles, reaching 87.3 mm in the last cycle. Table 1 presents the maximum mid-span deflection measured during each cycle, the residual deflection at the end of the cycle, the cumulative residual deflection prior to the cycle (the summation of the residual deflections from each preceding cycle) and the cumulative maximum deflection (the summation of the maximum deflection in the cycle and the cumulative residual deflection). During the final cycle the beam reached a total cumulative deflection of 215 mm (approximately span/50). Relative to the beam span, this is twice as large as the maximum deflection in the cellular beam test by Sheehan et al. (2016), in which the maximum vertical deflection was about span/100. The failure load of the beam was 18 kN/m^2, reached during the final cycle. This failure load did not include the weight of the spreader beam system (0.6 kN/m^2) and the self-weight of the composite beam (3.0 kN/m^2). Therefore the total load at failure reached 21.6 kN/m^2 including the self-weight and spreader beam system.

Table 1 Deflection (mm) at mid-span (LVDT-5) observed in the uniformly distributed load test

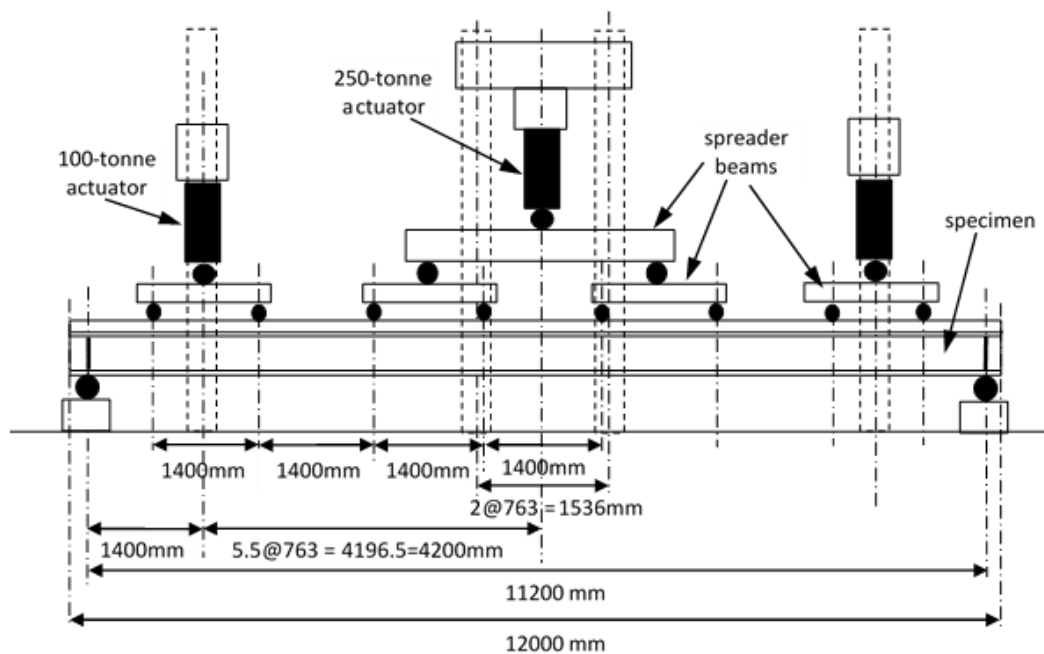| Load (kN/m^2)	3.0	5.0	7.5	10.0	12.0	15.0	18.0(Failure)
Maximum deflection in loading cycle	11.2	16.4	26.7	37.4	50.9	72.3	182.1
Residual deflection in individual loading cycle	3.1	2.1	3.5	5.2	7.8	11.2	87.3
Cumulative residual deflection before this individual loading cycle	0	3.1	5.2	8.7	13.9	21.7	32.9
Cumulative maximum deflection	11.2	19.5	31.9	46.2	64.8	94.0	215.0

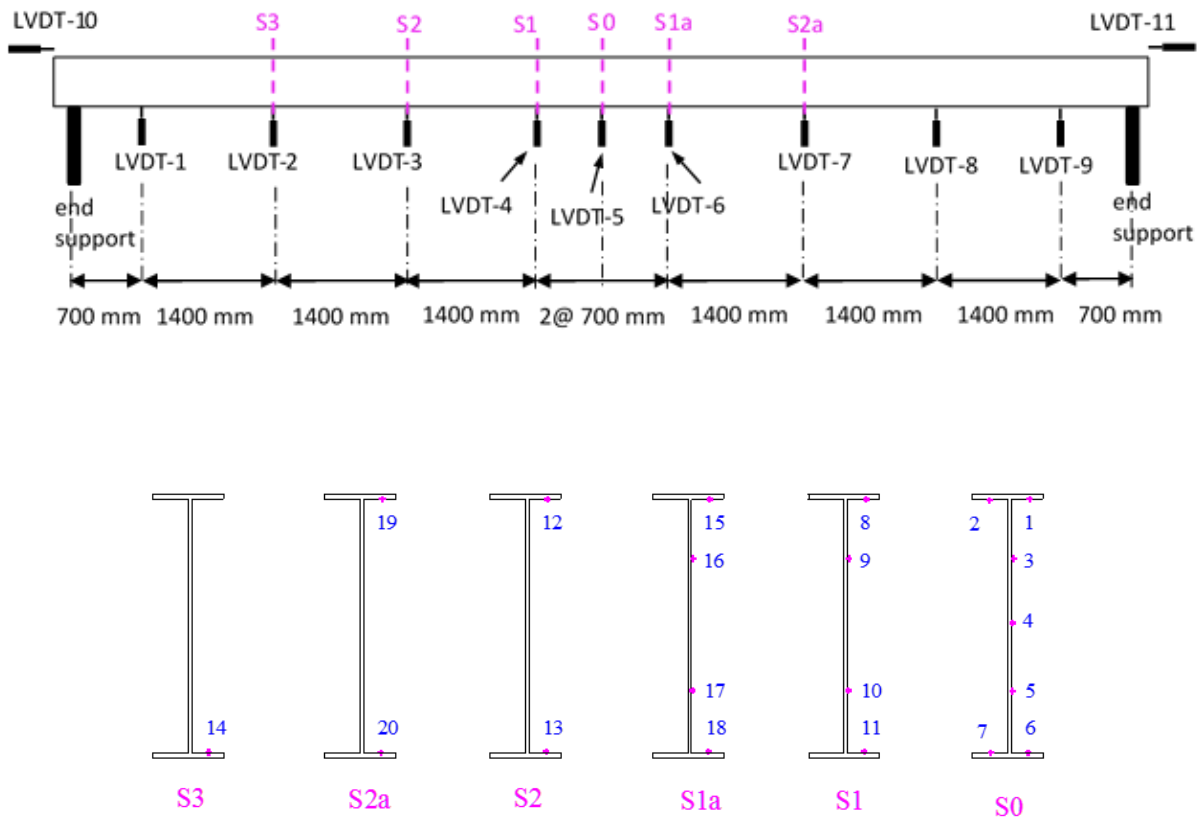Fig. 5 Arrangement of actuators and load-spreading beams

Fig. 6 Positions of LVDTs along specimen length and strain gauges on steel cross-section

Residual deflection = deflection on unloading after each load cycle. The relationship between load and vertical deflection for each cycle is shown in Figure 7. The relationship between load and deflection was almost linear up to a load of 8 kN/m^2, but became nonlinear as the load increased beyond this. The horizontal axis in this figure shows the total cumulative deflection during each cycle. The residual deflections were relatively small at the end of the first 6 cycles (up to 11.2 mm) but grew significantly in the last cycle (up to 87.3 mm).
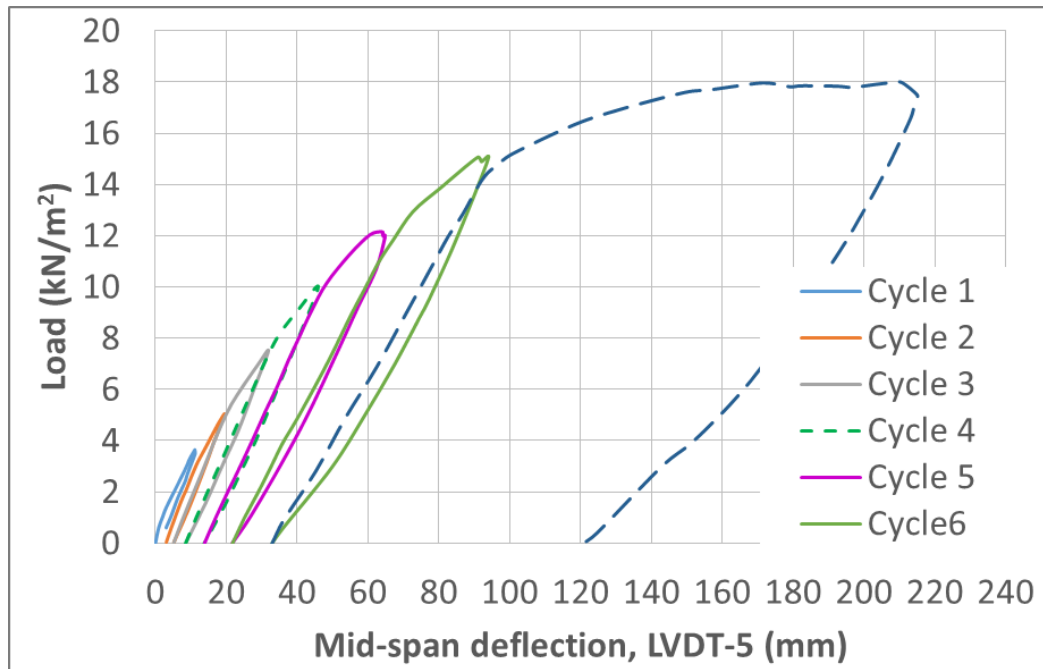
Fig. 7 Relationship between load and mid-span deflection

3.2 End-slip between concrete and steel

The end-slip measured by LVDT-11 for each loading cycle is shown in Table 2. In a similar manner to Table 1, the maximum end-slip in the cycle, residual end slip, cumulative residual slip and cumulative maximum slip are shown. The maximum end slip per cycle and residual slip increased slightly per cycle, reaching 4.62 mm and 1.20 mm respectively during the 6th cycle. During the final cycle, a maximum slip of 16.87 mm which amounted to a total cumulative end-slip of 19.21 mm. The residual end-slip at the end of the cycle was 9.68 mm. Despite these notable end-slip values, no shear stud failed during the test. According to Eurocode 4 Clause 6.6.1.1, in order for the behaviour to be classified as ductile, a specimen should have a minimum slip capacity of 6 mm. This is significantly lower than the measured slip values for the test specimen. The relationship between load and end-slip is shown in Figure 8. The relationship was fairly linear up to a load of 8 kN/m^2, after which it became increasingly non-linear.

3.3 Measured strains in steel flanges and concrete

Table 3 presents the strains measured in the steel top flange (S1), steel bottom flange (S6) and the top surface of the concrete slab (SC2). Negative values indicate compressive strain and positive values indicate tensile strain. The maximum cumulative strains in the top and bottom flanges of the steel section before the

last cycle were -531 με and 2186 με respectively. The yield strains in the top and bottom flanges were 2095 με and 1905 με respectively (corresponding to the measured yield stress values of 440 N/mm^2 and 400 N/mm^2). Hence, the bottom flange was beginning to yield at this stage, which the strain in the top flange was significantly below the yield strain. Both the top and bottom flanges exhibited large strains during the final cycle: 3 to 4 times the yield strain. The maximum accumulated strain in the concrete was −1156 με, which was just over half of the value (-2000 με) that would typically correspond to the maximum load for concrete.
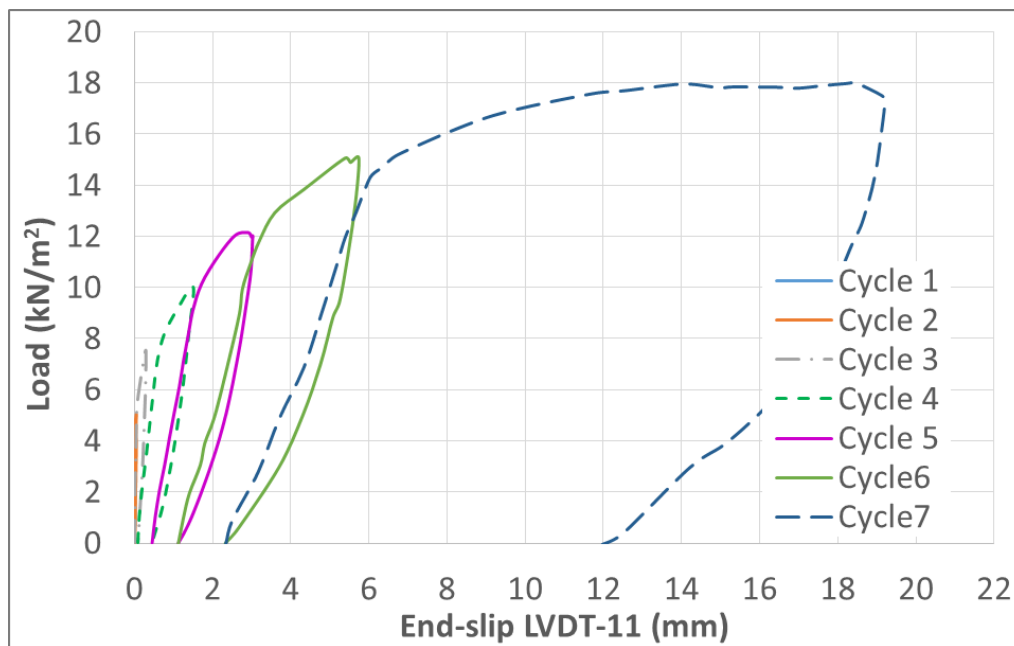

Fig. 8 Relationship between load and end-slip

Table 2 End slip (mm) between slab and steel beam observed in the uniformly distributed load test

Load (kN/m^2)	3.0	5.0	7.5	10.0	12.0	15.0	18.0(Failure)
Maximum end-slip in loading cycle	0.017	0.045	0.27	1.41	2.58	4.62	16.87
Residual end-slip in individual loading cycle	0.005	0.005	0.08	0.36	0.67	1.20	9.68
Cumulative residual slip before this individual loading cycle	0	0.017	0.02	0.10	0.46	1.13	2.34

Cumulative maximum slip	0.017	0.062	0.30	1.52	3.04	5.75	19.21

Table 3 Measured strains (με) in the steel flanges and the top surface of the concrete slab

Load (kN/m^2)	3.0	5.0	7.5	10.0	12.0	15.0	18.0
Maximum strain in top flange (S1) in this load cycle	-4	-10	-40	-86	-217	-427	-6160
Residual strain (S1) after this cycle	2	7	-4	-25	-84	-149	-5279
Cumulative residual strain (S1) before this cycle	0	2	9	5	-20	-104	-253
Total cumulative strain at (S1)	-4	-8	-31	-81	-237	-531	-6413
Maximum strain in bottom flange (S6) in this load cycle	362	501	758	1003	1228	1609	7781
Residual strain (S6) after this cycle	111	74	104	130	160	226	5868
Cumulative residual strain (S6) before this cycle	0	111	184	288	418	578	804
Total cumulative strain (S6)	362	612	943	1291	1646	2186	8585
Maximum strain in concrete slab mid-span (SC2) in this load cycle	-149	-225	-347	-457	-547	-671	-997
Residual strain (SC2) after this cycle	-32	-18	-25	-38	-27	-19	-209
Cumulative residual strain (SC2) before this cycle	0	-32	-49	-75	-113	-140	-159

$\mu = 10^{-6}$ or micro strain

Table 4 Deflection (mm) at mid-span (LVDT-5) observed in the uniformly distributed load test

Top flange				Bottom flange			
Point ID	Distance from support (mm)	Strain with previous residual strain	Strain without previous residual	Point ID	Distance from support (mm)	Strain with previous residual strain	Strain without previous residual
				14	2100	1519	1203
12	3500	-1681	-1403	13	3500	4395	3583
8	4900	-925	-701	11	4900	2852	2269
1	5600	-5687	-5434	6	5600	7859	7055
2	5600	-1906	-1696	7	5600	1989	1350
15	6300	-3479	-3175	18	6300	10829	10459
19	7700	-	-	20	7700	3295	2755

Figures 9-11 depict the relationship between load and strain in the top flange, bottom flange and concrete. The relationship between load and strain in the steel flanges was close to linear under low loads (less than 10 kN/m^2) and became increasingly nonlinear under higher loads (greater than 10 kN/m^2). Although the top flange exhibited very high compressive strains in the final cycle, no buckling was observed.

The measured strains at different positions along the beam top flange and bottom flange are displayed in Table 4 at the failure load. The strains are presented both with and without the previous residual strain and are arranged in the table in relation to their distance from the end support, with the mid-span located at 5600 mm from the support. Values of strain in the top flange (left hand side of table) are all negative,

indicating compression, with the highest value at the mid-span. The strains at positions 12 and 8 are approximately half of the magnitude of those at positions 15 and 19, which are in the equivalent points on the opposite side of the span. The highest tensile strain in the bottom flange occurred at point 18, 6300 mm from the end support. Hence the overall behaviour of the beam was not symmetric about the mid-span during the final cycle of the test. At points 13, 11, 6, 7, 18 and 20 the cumulative tensile strains exceeded the yield strain (1905 με) Only point 14, the closest to the end support, did not reach yield in tension. In compression, the steel top flange reached yield (2095 με) at the mid-span and at point 15. Table 5 presents the strains at different cross-sections along the beam length, where the positions of cross-sections S0, S1, S2, S3, S1a and S3a are illustrated in Figure 6. At the mid-length (S0) the strains at positions 1 and 6, in the top and bottom flanges on one side of the beam, are approximately 4 times greater than at positions 2 and 7, at the other side, suggesting that twisting or out-of-plane bending of the beam took place. Strains were measured in the web at sections S0, S1 and S1a.   In each of these sections, low compressive strains were observed in the upper portion of the web while larger tensile strains (exceeding yield) were measured in the lower portion of the web, implying that the neutral axis of the section in bending was located in the upper half of the steel beam web.
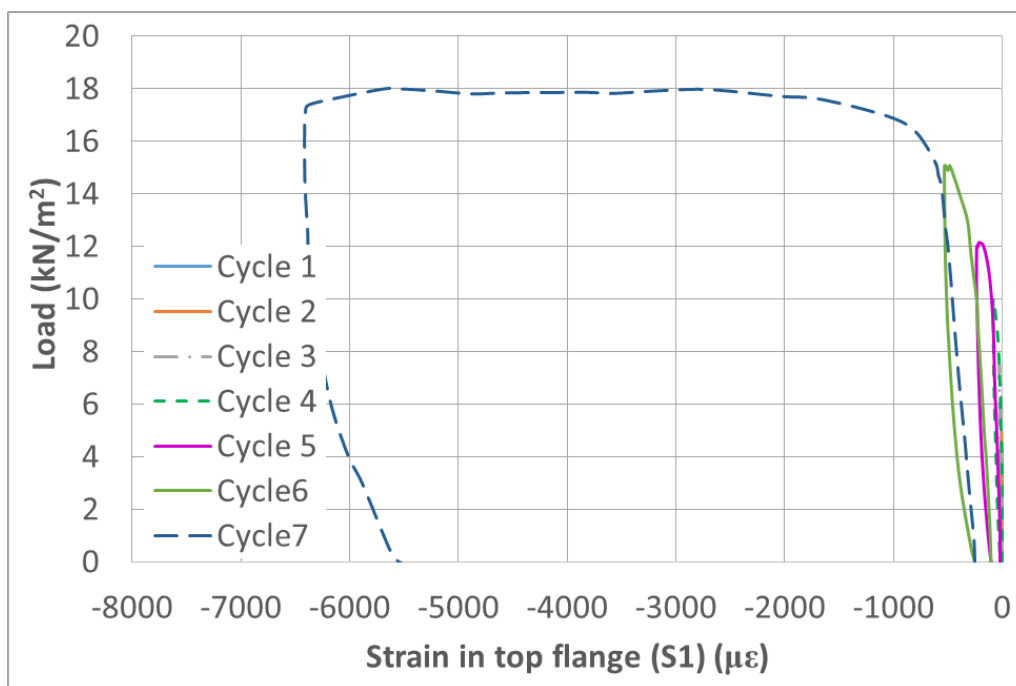

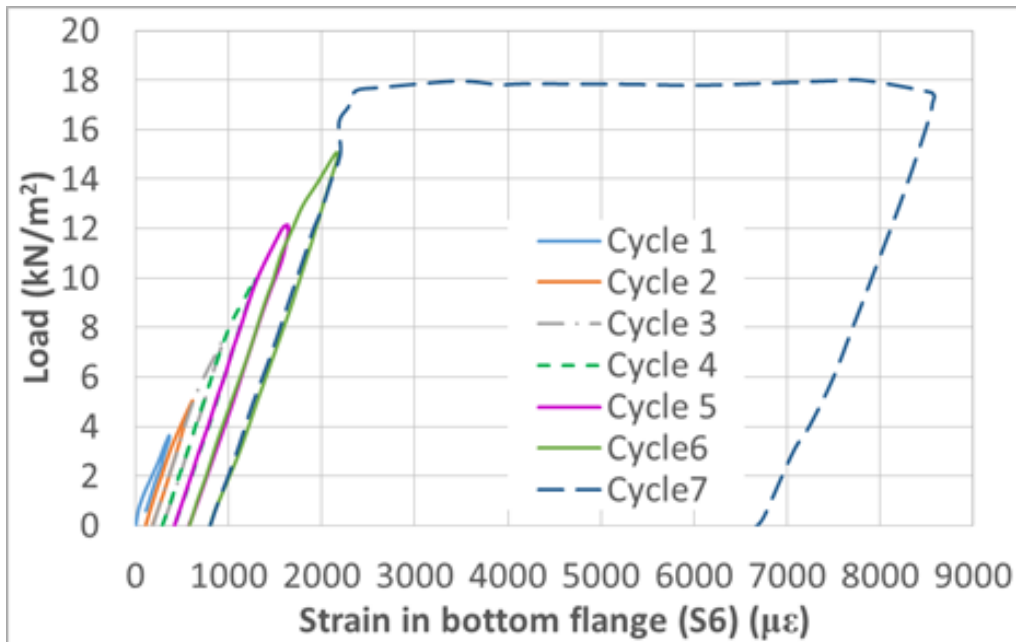Fig. 9 Relationship between load and strain in top flange

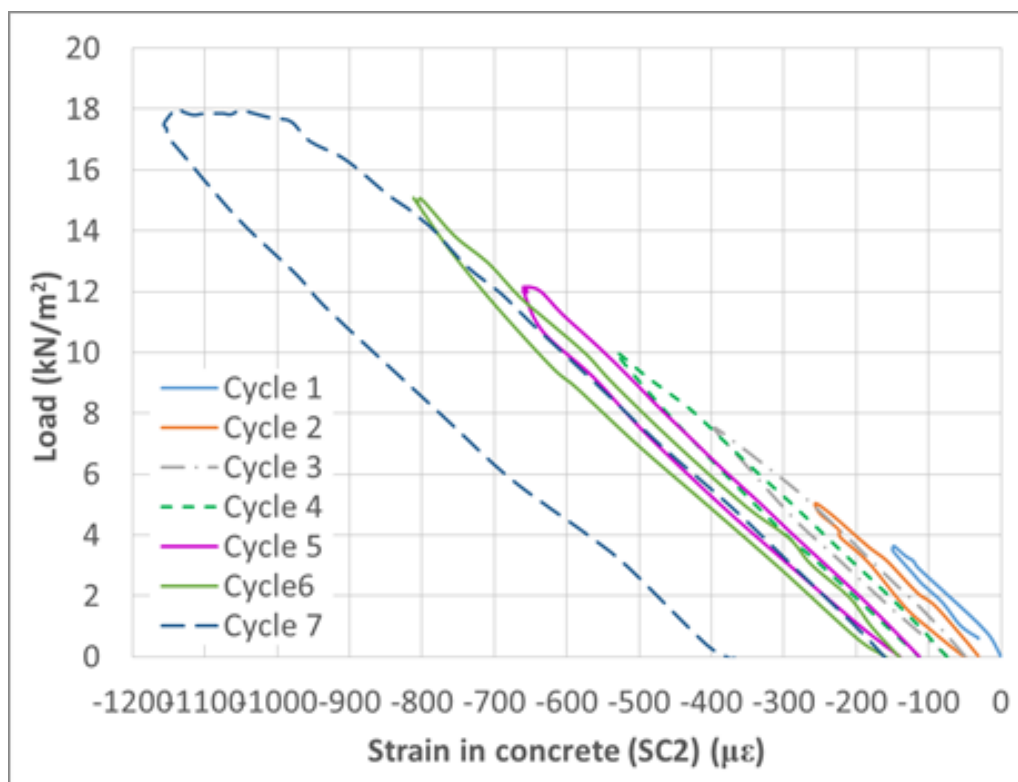Fig. 10 Relationship between load and strain in bottom flange

Fig. 11 Relationship between load and strain in concrete

3.4 Mode of failure

After the experiment, the concrete slab and decking were cut and the cells in the composite deck were numbered from 1 (at the beam end) to 37 (at the opposite end). Some of these are shown in Figure 12. In

most cells, longitudinal cracking was observed at the level of the shear stud/top of the trough. However, unlike the composite cellular beam previously tested by Sheehan et al. (2016), no concrete crushing occurred. Failure was deemed to have occurred through yielding of the steel beam, which is confirmed by the very high strains that were measured in the steel.

4 Analysis and Discussion

4.1 Shear stud capacity and degree of Shear Connection

In previous push-out tests conducted by Nellinger et al. (2017) using C30 concrete, the shear stud capacity was found to be 75 kN. Hence for concrete with a strength of 25 N/mm^2 the shear stud capacity was estimated to be $75 \times (25/30)^{1/2} = 68$ kN.

Using this value for shear stud resistance assessment, the degree of shear connection, η, was calculated by:

$$\eta = n/n_f \tag{1}$$

where n_f was the number of connectors for full shear connection

and n was the number of connectors provided.

η was calculated to be 33 %.

In Eurocode 4, the minimum required degree of shear connection depends on the bottom flange area/top flange area ratio, the material strength and the member length. For steel sections with equal flanges, used as simply supported beams with a span not exceeding 25 m, the degree of shear connection is calculated by

$$\eta \geq 1 - \left(\frac{355}{f_y}\right)(0.75 - 0.03L_e), \eta \geq 0.4 \tag{2}$$

For steel sections with a bottom flange area to top flange area ratio of 3, used as simply support beams with a span not exceeding 20 m, the degree of shear connection is calculated by

$$\eta \geq 1 - \left(\frac{355}{f_y}\right)(0.30 - 0.015L_e), \eta \geq 0.4 \tag{3}$$

as stated by Clause 6.6.1.2 in Eurocode 4. L_e is the span (or distance between points of zero bending) and f_y is the steel yield strength. According to this clause, η must not be below 40%. Lawson and Saverirajan

(2011) recognised that a lower degree of shear connection may be permissible in beams using unpropped construction and recommended using a reduction factor of $(M/M_{\text{pl}})^{1.5}$ for the minimum degree of shear connection in these cases, where M is the applied bending moment. Lawson and Saverirajan (2011) also recommended keeping the degree of shear connection above 40%. The required degree of shear connection according to the Eurocode 4 guidelines was calculated to be 77% for the tested beam. Hence the actual degree of shear connection was considerably below this and even below the minimum of 40 %. If pairs of shear connectors had been used instead of single shear connectors, the degree of shear connection (calculated using Clause 6.6.3.1 and the reduction factor in Clause 6.6.4.2 of EN 1994-1-1) would still have been significantly lower than the degree required by Eurocode 4.

4.2   Moment Capacity

The moment capacity of the cross-section was calculated in accordance with Clause 6.2.1.3 of Eurocode 4. Assuming a plastic stress distribution for the steel and concrete and using the measured steel yield stress value, the plastic bending resistance was estimated to be 965 kNm. For a uniformly distributed load w, the bending moment at the mid-span of a beam of length L is $wL^2/8$. The maximum applied load in the test was 21.6 kN/m^2 (18.0 kN/m^2 from actuators plus 3.6 kN/m^2 from beam and spreader self-weight), which corresponded to an applied bending moment of 948 kNm ($21.6 \times 2.8 \times 11.2^2/8$) at the mid-span. This was less than 2% lower than the applied bending resistance, showing that the bending resistance of the test specimen agreed closely with the Eurocode 4 prediction. The good correlation in the result also confirmed the previously calculated shear stud resistance (68 kN) and degree of shear connection.

Table 5 Measured strains in different sections at the maximum load 18 kN/m^2

Section ID	Monitoring point ID	Monitoring point position	Strain with previous residual	Strain without previous residual
S0	1	top flange	-5687	-5434
	2	top flange	-1906	-1696
	3	web	-213	-248
	4	web	1482	1209
	5	web	2737	2231
	6	bottom flange	7859	7055
	7	bottom flange	1989	1350
S1	8	top flange	-925	-701
	9	web	-81	-81
	10	web	2964	2260
	11	bottom flange	2852	2269
S2	12	top flange	-1681	-1403
	13	bottom flange	4395	3583
S3	14	bottom flange	1519	1203
S1a	15	top flange	-3479	-3175
	16	web	-570	-563
	17	web	5908	5126
	18	bottom flange	10829	10459
S2a	19	top flange	-	-
	20	bottom flange	3295	2755

Fig 12 Concrete slab of solid-web composite beam after testing and cutting

4.3 Strain distribution

As discussed previously, the strains in the steel beam were measured during the casting of the concrete. Figures 13 and 14 depict the strains measured during the casting of the concrete in addition to the strains measured in the steel beam and concrete slab at the mid-span during the test. Figure 13 shows the steel flange strains on the left hand side of the beam (S2: top flange; S7: bottom flange) and Figure 14 shows the steel flange strains on the right hand side of the beam (S1: top flange; S6: bottom flange) during the test. The four strain gauges in the concrete had similar values and hence the same value was used in Figures 13 and 14. In each figure, the strains during casting are added to the strains measured during the test to give the total combined strain. Comparing the figures, it is evident that the steel on the right hand side underwent significantly larger strains than that on the left hand side. Overall, the strain distribution through the section depth is similar to that proposed by Seracino et al. (2001), for composite beams with partial shear connection.
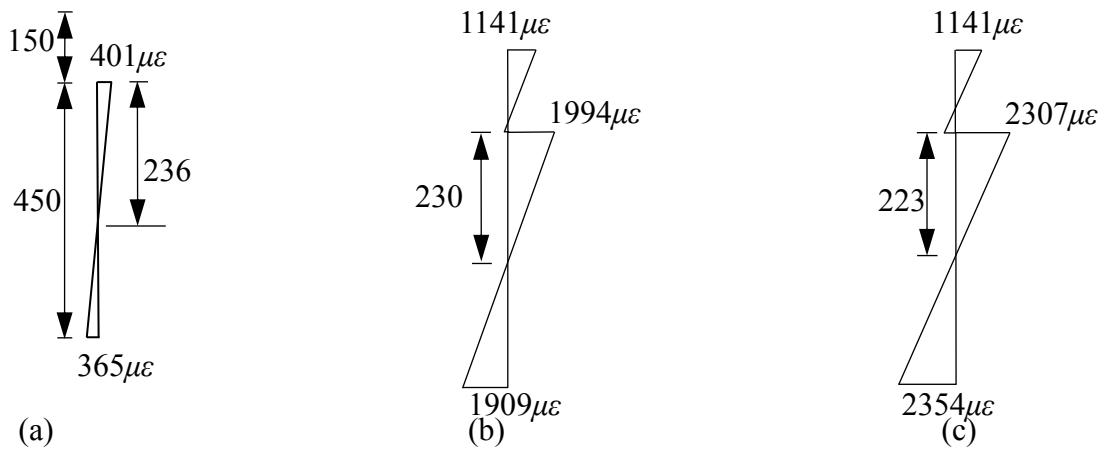
Fig 13 Strain distribution through cross-section corresponding to measured strains S2 and S7: (a) during concrete pour; (b) measured during test; (c) combined strains
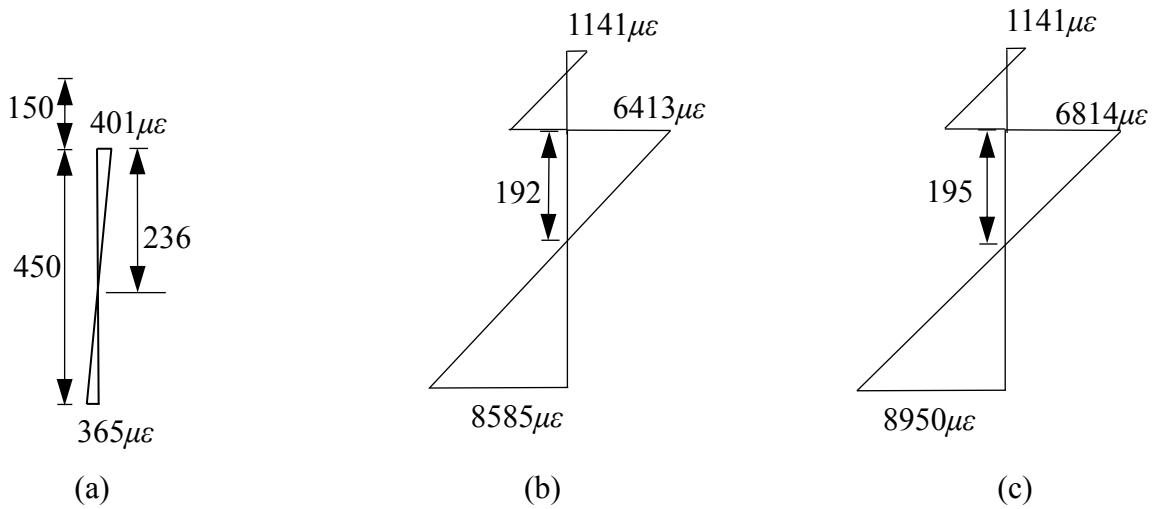

Fig 14 Strain distribution through cross-section corresponding to measured strains S1 and S6: (a) during concrete pour; (b) measured during test; (c) combined strains

The position of the neutral axis was estimated by assuming a linear strain variation through the depth of the beam. The addition of the residual strain had little influence on the position of the neutral axis, which was 223 mm from the top of the LHS of the section and 195 mm from the top of the RHS of the beam section. The estimated strains in the centres of the top and bottom flanges (average strains of S1 and S2; S6 and S7) are presented in Figure 15 along with the strains measured in the web (S3-S5). Figure 15 presents a simplified multi-linear diagram based on the strains measured at monitoring points throughout the section.

The position of the neutral axis using the strains measured in the web is higher than that estimated using only the flange strains, at 144 mm below the upper surface of the top flange. These are only estimated values however, since the strain variation through the section depth was actually highly nonlinear in reality, with large plastic strains in the vicinity of the flanges.
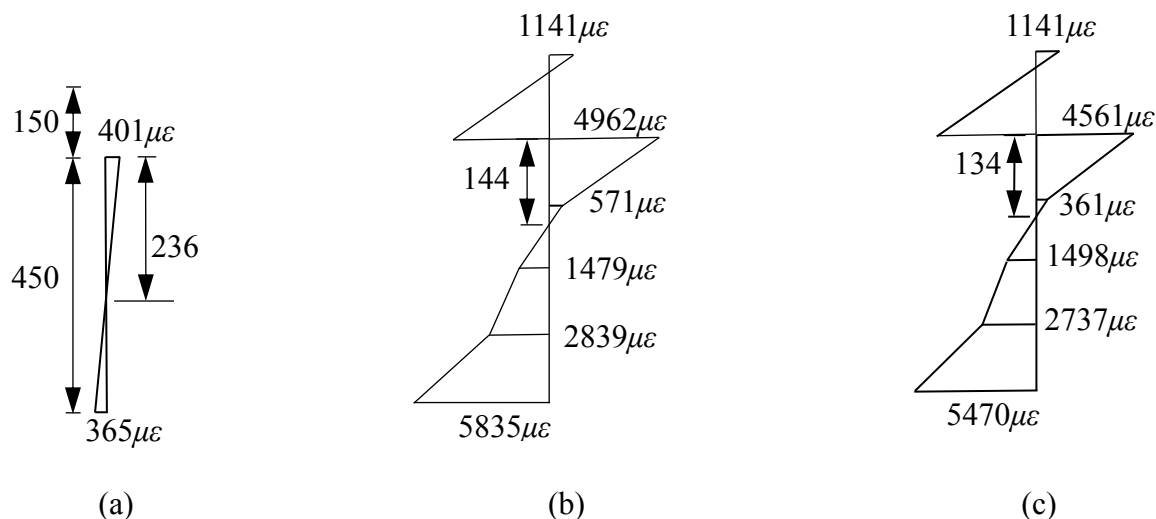

Fig 15 Strain distribution through cross-section depth corresponding to measured strains S3-S5 (web) and average measured flange strains

The estimated height of the neutral axis for each cycle of the test is shown in Table 6, based on the strain gauge readings S1 and S6 in the top and bottom flanges. The neutral axis appears to move upwards during the first four cycles and then downwards during the last 3 cycles. It is worth noting that the estimated neutral axis positions were calculated using the combined strains measured during the pouring of the concrete and the composite beam test. For the first four cycles, very low strains were measured in the top flange of the steel, with the residual strain from the concrete pour accounting for most of the strain. Without the inclusion of this residual strain, the neutral axis would appear to be close to the top of the steel beam, or in the concrete slab, based on the measured strain values.

Table 6: Estimated neutral axis position for each cycle under uniformly distributed load

Without residual strain from concrete pour		Considering residual strain from concrete pour	
Load	Neutral axis depth from top of steel beam	Load	Neutral axis depth from top of steel beam
3.5 kN/m²	5 mm	3.5 kN/m²	161 mm
5.0 kN/m²	6 mm	5.0 kN/m²	133 mm
7.5 kN/m²	14 mm	7.5 kN/m²	112 mm
10.0 kN/m²	27 mm	10.0 kN/m²	101 mm
12.0 kN/m²	57 mm	12.0 kN/m²	108 mm
15.0 kN/m²	88 mm	15.0 kN/m²	120 mm
18.0 kN/m²	193 mm	18.0 kN/m²	195 mm

The position of the elastic neutral axis is calculated using

$$y_e = \frac{A_{bf}\,y_{bf} + A_{tf}\,y_{tf} + A_w\,y_w}{A_{bf} + A_{tf} + A_w} \tag{4}$$

where A_{bf}, A_{tf} and A_w refer to the areas of the bottom flange, top flange and web respectively. y_{bf}, y_{tf} and y_w represent the distance between the top of the beam and the centroid of each of these areas. For the steel beam elastic neutral axis was calculated to be 242 mm from the top of the section, which is close to the position indicated by the strain measurements taken during the pouring of the concrete. The position of the elastic neutral axis for the composite section was calculated by using an equivalent steel area for the concrete and a modular ratio of 6 between the material stiffness values, and was found to be located in the concrete slab, 120 mm above the top of the steel beam. This corresponds to the very low strains measured in the top flange. The position of the plastic neutral axis was computed using plastic stress blocks and the measured material properties and was calculated to be in the steel beam web at a position of 131 mm below the top of the steel flange. The neutral axis positions estimated from the measured strains were between the elastic and plastic neutral axis positions for most cycles, except for the last cycle, when it is lower than the plastic neutral axis.

4.4 Vertical Deflection

The second moment of area for the fabricated steel beam was simply 263×106 mm^4 while the second moment of area of the composite beam was 1104×106 mm^4. The expected mid-span deflection δ for a beam subjected to uniformly distributed load w is given by

$$\delta = 5wL^4/384EI \qquad (5)$$

where L is the span of the beam, E is the modulus of elasticity of the material and I is the second moment of area. This formula was used to predict the deflection of the steel beam during pouring of the concrete and the deflections of the composite beam under each cycle of the uniformly distributed load, the effective second moments of area, I_{eff}. The results are presented in Table 7 and compared with the vertical deflections measured during the tests, omitting the residual deflections from the previous loading cycles.

The predicted deflection during pouring of the concrete (27 mm) was close to the actual (23 mm). For the composite section, the predicted deflection during the early loading cycles was slightly lower than the actual deflection, but this difference increased in subsequent cycles, to an even greater extent than for the cellular beam. As the steel strains exceeded the elastic limit and the response became increasingly nonlinear, the final cumulative deflection was more than 4 times greater than the prediction based on elastic behaviour.

Table 7 Predicted and actual mid-length vertical deflections

Stage/Cycle	I_{eff} (mm^4)	$\delta_{predicted}$ (mm)	δ_{actual} (mm)
2.5 kN/m^2 (concrete pour)	275×10^6	26	23
3.5 kN/m^2	1148×10^6	9	11
5.0 kN/m^2	1148×10^6	12	16
7.5 kN/m^2	1148×10^6	19	27
10.0 kN/m^2	1148×10^6	25	37
12.0 kN/m^2	1148×10^6	30	51
15.0 kN/m^2	1148×10^6	37	72
18.0 kN/m^2	1148×10^6	45	182

BS5950-3-1 provides the following formula to calculate the deflection of a composite beam with a partial degree of shear connection:

$$\delta = \delta_c + 0.3(1-N_a/N_p)(\delta_s - \delta_c) \tag{6}$$

where δ_c is the deflection of the beam with full shear connection, δ_s is the deflection of the steel section alone, N_a is the number of shear connectors between the intermediate point and the support and N_p is the number of shear connectors required between the intermediate point and the support in order for positive moments to occur.

Figure 16 compares the measured mid-span deflection with two different approaches for predicting the value. The first set of predictions is computed using Equation (5). The deflection is calculated assuming full shear connection between the steel and concrete (reflected in the '*EI* 'value) and no shear connection, and using these two cases, a third case is obtained for 33% shear connection by linear interpolation. The second approach is carried out using Equation (6), taken from BS5950-3-1. The figure demonstrates that BS5950 provides a closer prediction to the test results up to a load of 40 kN/m, after which the deflection became very large, and the specimen response was increasingly non-linear. The interpolation approach tended to overestimate the mid-span deflection for most phases of the test. Since the mid-span deflections are generally expected to be within the elastic range for design applications, the formula provided in BS5950 is deemed to be satisfactory.
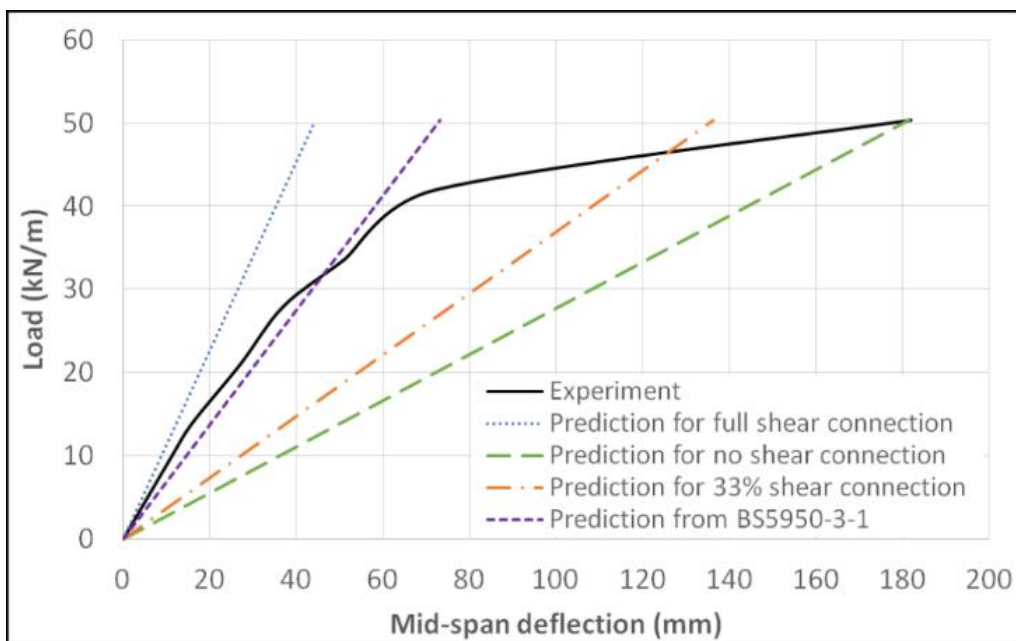

Fig 16 Estimations for mid-span deflection during test

5   Conclusions

A series of experiments has been conducted to explore the response of an unpropped, composite beam with a low degree of shear connection under uniformly distributed load. The findings are summarised as follows:

- Under uniformly distributed loading, the section achieved its plastic moment capacity, despite having a degree of shear connection considerably below the minimum Eurocode 4 requirements outlined in Clause 6.6.1.2. This suggests that the rules for the minimum degree of shear connection could be relaxed.

- No concrete crushing was observed, only a longitudinal crack occurred at the level of the shear connectors along the beam length. The beam failed by yielding of the steel. The tensile strains measured in the bottom flange were several times greater than the strain corresponding to first yield, for a considerable portion of the beams length. Large compressive strains exceeding the yield strain were also observed in the top flange of the beam.

- Ductile behaviour of the shear connectors was confirmed when an end slip of 19.2 mm was measured during the test, exceeding the 6 mm limit by Eurocode 4 Clause 6.6.1.1. No shear connector failed during the test.

- The beam exhibited a mid-span vertical deflection of L/50 before a reduction occurred in the load-carrying capacity. This corresponded to a load of 18 kN/m^2, reinforcing the argument for modifying the design load recommendations for these types of composite beams.

- The vertical deflections of the beam were generally underestimated by the equation $\delta = 5wL^4/384EI$, but the formula $\delta = \delta_c + 0.3(1-N_a/N_p)(\delta_s - \delta_c)$ provided in BS5950 produced a reliable prediction.

The findings suggest that Eurocode 4 design recommendations could be modified to better exploit the properties of unpropped composite beams, particularly with regard to the required degree of shear connection. Numerical analysis using the finite element software package ABAQUS will support the recommendations following from this research project.

6   Acknowledgement

References

Banfi, M. (2005), "Slip in composite beams using typical material curves and the effect of changes in beam layout and loading", *Engineering Foundation Conference V*, South Africa.

BS 5950-3-1 (1990), "Structural use of steelwork in building. Design in composite construction", BSI.

Durif S, Bouchair A and Vassart O. (2013), "Experimental tests and numerical modeling of cellular beams with sinusoidal openings", *Journal of Constructional Steel Research*, 82, 72-87.

EN 1994-1-1. Eurocode 4 (2004). Design of composite steel and concrete structures – Part 1-1: General rules and rules for buildings, Brussels, Belgium.

Erdal F and Saka MP (2013), "Ultimate load carrying capacity of optimally designed steel cellular beams", *Journal of Constructional Steel Research*, 80, 355-68.

Lam, D. (2007), "Capacities of headed stud shear connectors in composite steel beams with precast hollowcore slabs", *Journal of Constructional Steel Research,* 63(9), 1160-1174.

Lawson, R.M., Lim, J., Hicks, S.J. and Simms, W.I. (2006), "Design of composite asymmetric cellular beams and beams with large web openings", *Journal of Constructional Steel Research,* 62(6), 614-629.

Lawson, R.M. and Saverirajan, A.H.A. (2011), "Simplified elasto-plastic analysis of composite beams and cellular beams to Eurocode 4", *Journal of Constructional Steel Research,* 67(10), 1426-1434.

Luo Y, Li A and Kang Z. (2012), "Parametric study of bonded steel-concrete composite beams by using finite element analysis", *Engineering Structures,* 34, 40-51.

Nellinger, S., Odenbreit, C., Obiala, R., Lawson, M. (2017), "Influence of transverse loading onto push-out tests with deep steel decking", *Journal of Constructional Steel Research*, 128, 335-53.

Papastergiou, D. and Lebet, J-P, (2014), "Design and experimental verification of an innovative steel-concrete composite beam", *Journal of Constructional Steel Research* 93, 9-19.

Qureshi J, Lam D. and Ye J (2011), "Effect of shear connector spacing and layout on the shear connector

capacity in composite beams", *Journal of Constructional Steel Research*, 67(4), 706-19.

Ranzi, G., Bradford, M.A., Ansourian, P., Filonov, A., Rasmussen, K.J.R., Hogan, T.J. and Uy, B. (2009), "Full-scale tests on composite steel-concrete beams with steel trapezoidal decking", *Journal of Constructional Steel Research,* 65(7), 1490-1506.

Seracino, R., Oehlers, D. J., Teo, M. F. (2001), "Partial-interaction flexural stresses in composite steel and concrete bridge beams", *Engineering Structures*, 23, 1186-93.

Sheehan, T., Dai, X.H., Lam, D., Aggelopoulos, E., Lawson, M. and Obiala, R., (2016), "Experimental study on long spanning composite cellular beam under flexure and shear", *Journal of Constructional Steel Research*, 116, 40-54.

Zona A and Ranzi G (2014), "Shear connection slip demand in composite steel-concrete beams with solid slabs", *Journal of Constructional Steel Research,* 102, 266-81.